JOURNAL DE PHYSIQUE
Colloque C7, supplément au n°9, Tome 45, septembre 1984

STRUCTURE AND DYNAMICS OF THE HYDROGEN BOND NETWORK IN WATER BY COMPUTER SIMULATIONS

A. Geiger, P. Mausbach, J. Schnitker, R.L. Blumberg* and H.E. Stanley*

Institut für Physikalische Chemie, Rheinisch-Westfälische Technische Hochschule Aachen, D-5100 Aachen, F.R.G.
**Center of Polymer Studies and Department of Physics, Boston University, Boston, Massachusetts 02215, U.S.A.*

Résumé - Nous résumons les résultats obtenus précédemment par notre analyse du réseau des liaisons hydrogène dans l'eau pure et nous discutons l'influence de la température à densité constante dans la région du liquide en surfusion. Une très faible dépendance en température des propriétés d'une liaison simple est opposée à des effets fortement dépendants de la température sur les propriétés statiques et dynamiques, qui sont déterminées par l'influence collective de plusieurs liaisons. De plus, l'existence d'un minimum du facteur de structure S(Q) à faible vecteur d'onde Q a été trouvée pour le liquide modèle, indiquant la présence de fluctuations de densité ayant des longueurs de corrélation de plusieurs diamètres moléculaires.

Abstract - We summarize previous results of our hydrogen bond network analysis on pure water and discuss the influence of temperature at constant density in the region of the supercooled liquid. A very weak temperature dependence of the single bond properties is contrasted by marked temperature effects on static and dynamic properties, which are determined by the collective influence of many bonds. Also, the existence of a minimum in the structure factor S(Q) at low wave vectors Q was found for the model liquid, indicating the presence of density fluctuations with correlation lenghts of several molecular diameters.

I - INTRODUCTION

The investigation of the supercooled range of liquid water has stimulated the proposition of several new structural models of water to explain the unusual behavior of this liquid /1-7/. Although, in most of these attempts, the connectivity of the hydrogen bond network plays a central role, there is no possibility for a direct experimental determination of extended hydrogen bond network structures. Therefore it seems to be appropriate to use computer simulation of liquid water to get information about bond networks and to test the assumptions of the proposed models.

Already in their first molecular dynamics simulation study of water, Rahman and Stillinger calculated the number of hydrogen bonds exhibited by single water molecules /8,9/. Later, the occurence of bond rings /10/ and larger bond aggregates was investigated and the existence of a bond percolation threshold could be demonstrated /11/.

Coincidently, the more recent models explain the apparent singular behavior of water near its supercooling limit by the existence of structural units, which are imbeded in the bond network and whose

occurence probability is growing in a self-amplifying manner, when the temperature is decreased. The suggested underlying growth mechanisms and the corresponding structural units are characterized by catchwords like the "percolation of correlated four-bonded sites" /4/, the "aggregation and mutual stabilization of bulky polyhedra" /5,6/, or the "self replication of pentagonal rings" /7/.

In the present contribution we report results of a current project aimed to investigate the hydrogen bond network by the use of molecular dynamics (MD) simulation; one of the focal points being the test of assumptions and consequences of the percolation model of water.

II - SUMMARY OF PREVIOUS RESULTS

Most of the hydrogen bond network analysis results, which have been published by us up to now, had been obtained for a system of 216 water molecules interacting via an ST2 pair potential; density and temperature being ϱ = 1.0 g/cm³ and T = 284 K. The input data for our calculations are configurations from a corresponding MD simulation by Rahman and Stillinger /9/.

Our results support the following picture: (a) instantaneous snapshots show water as a macroscopic, space-filling gel-like (transient) network of hydrogen bonds; (b) this bond network contains small regions (patches) of increased connectivity and decreased local density. The first statement could be deduced from the observation of a bond percolation threshold, which is situated in quantitative agreement with random bond percolation theory at an average number of hydrogen bonds per molecule of $\langle n_{HB} \rangle$ = 1.53. All reasonable estimates for this quantity from experiments give higher values, indicating thus the existence of an infinite bond network in real water /11,12/.

The second statement is supported by the observation of strong correlations between the degree of bondedness of the molecules and the local density: It could be shown that local density is decreased in the vicinity of those water molecules, which have four intact hydrogen bonds /13/. Moreover we could demonstrate a more general correlation between the number of molecules within a sphere of radius R_c around a given molecule and the total interaction energy of that molecule with its neighbors residing in that sphere (its "binding energy") : In contrast to the behavior of a normal fluid, for most choices of R_c the energy increases (becomes less negative) when more molecules are in the sphere, thus favouring energetically a loose packing of water molecules /12/. The existence of these patches of low local density is also in agreement with recent small angle x-ray scattering data for supercooled water /14/.

To get a more detailed and quantitative description of the hydrogen bond network, we calculated distribution functions giving the weight fraction W_M^N of water molecules which belong to "nets" of M molecules. Likewise we determined the corresponding weight fraction W_s^C of molecules, belonging to "patches" or "clusters" of s connected water molecules, which all have four intact hydrogen bonds. It is striking to see the degree of quantitative agreement - without any adjustable parameters - between the MD simulation results and the predictions of percolation theory, when using random bond percolation calculations for W_M^N and correlated-site percolation theory for W_s^C /12,15/. This is also true for properties like the mean cluster size, the percolation threshold and even the exponents characterizing the singular behavior at the percolation threshold /16/.

The percolation calculations have to be based on the connectivity of some lattice; we considered ice I_h and diamond. It turned out that within the accuracy of the present MD results the choice of the lattice is not crucial as long as there are four bonding possibilities per molecule and bond ring formation is allowed. The neglect of bond cycles, as in the case of the Cayley tree pseudolattice (corresponding to Flory theory of condensation), leeds to marked discrepancies already for small bond networks. Moreover in that case the predicted percolation point is in disagreement with the MD results /15/.

III - TEMPERATURE DEPENDENCE OF THE HYDROGEN BOND NETWORK STRUCTURE

III.1 MD simulation outline

To study the temperature behavior of the bond network, we performed a series of simulation runs with decreasing internal energies, keeping the density constant at $\rho = 1.0$ g/cm³ (with $N = 216$ particles in the periodically repeated box). Penetrating into the temperature region of supercooled water, we are faced with strongly increasing relaxation times and accordingly with strongly increasing lenghts of simulation runs and equilibration periods.

To save computer time, we reduced the cutoff radius for direct interactions to oxygen separations of $r_c = 7.8$ A. Two disadvantages of this procedure have to be considered: (a) a worsening of total energy conservation and connected with this an upward trend of the temperature, which is particularly untolerable in very long simulation runs, (b) an increased distortion of orientational correlation beyond the shell of nearest neighbors. These defects can be remedied by adopting the reaction field method, which had been examined for ST2-water by Steinhauser; we also included the use of its tapering function to smooth the cutoff /17/. By this we obtain a very good energy stability, comparable to Lennard-Jones system simulations; the usual temperature rescaling procedure could be avoided completely. Also, from the fluctuations of the total dipole moment of the systems, we can derive Kirkwood g-factors and static dielectic constants, which indicate the presence of more realistic long range orientational correlations than those found in the original simulation runs of Rahman and Stillinger.

Unfortunately, there are also two drawbacks of the reaction field application: (a) the pressure as calculated from the virial of intermolecular forces increases appreciably compared to that obtained with the simple cutoff procedure by Rahman and Stillinger, (b) the particle dynamics is accelerated, leading to increased self diffusion coefficients and decreased rotational correlation times, as will be discussed in chapter IV.

We performed a total of eight simulation runs with decreasing temperatures. The timestep size for the integration of the equations of motion was $\Delta t = 1.22 \cdot 10^{-15}$ sec. Fig. 1 illustrates the lenght of the individual runs, demonstrating excessively increasing equilibration times. Only during the shaded periods of lenght roughly 10 ps every eighth configuration was saved on tape and examined more extensively later on. The reported results always refer to the last of these periods. This procedure was due to the fact, that the simulation runs were performed on a VAX 780 with attached array processor FPS 164 in a special purpose configuration with very limited mass storage capabilities.

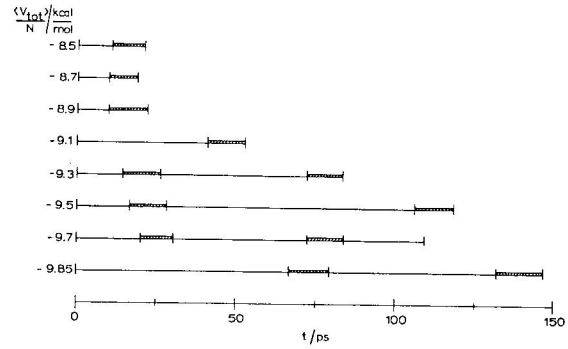

Fig. 1 - Lenght of simulation runs and periods of analysis (shaded).

III.2 Some macroscopic properties

In Table I some characteristic data of the simulation runs are collected. They were obtained as averages over the above mentioned time intervalls of about 10 ps and show appreciable scatter. This is a consequence of the increasing low-frequency fluctuations, we expect when cooling down the liquid.

E_{tot}/kcal mol^{-1}	-8.50	-8.70	-8.90	-9.10	-9.30	-9.50	-9.70	-9.85
$N_{analys.}$/ t	8200	7300	9900	9400	10300	10100	9600	12100
T / K	287	282	270	271	260	247	241	235
C_V / R	12.2	11.6	12.5	10.2	8.2	11.8	12.2	8.6
$W = \frac{p}{\rho kT} - 1$	-0.21	0.07	-0.02	0.28	0.23	0.31	0.47	0.62
$G_K = \overline{M^2} / N$	1.22	3.85	3.08	3.47	2.05	4.06	4.22	10.95
ϵ_r	36	116	96	109	67	139	148	393

Table I

None the less, there are quantities, which show a clear tendency: as temperature falls constantly with decaying total internal energy E_{tot} , the pressure rises, as indicated by the virial of intermolecular forces

$$W = \frac{p}{\rho k T} - 1 .$$

This corresponds to the well known decrease of the density at constant pressure. However, the pressures, calculated from the virials, are much too high ($\gtrsim 1$ kbar), as has been observed before, when applying reaction fields /18/.

Also the fluctuations $\overline{M^2}$ of the total dipole moment $\underline{M}$ show a tendency to increase with decreasing temperatures. $\underline{M}$ is given by

$$\underline{M} = \sum_{i=1}^{N=216} \underline{m}_i \quad ,$$

with $\underline{m}_i$ the unit vector in direction of the electric dipole moment of molecule i . For infinite systems

$$G_k = \overline{M^2} \; / \; N$$

has to approach the Kirkwood orientational correlation factor g_K. As we can see, by the application of the reaction field, G_K adopts the magnitude of the experimental g_K , in contrast to those values obtained in simulations without reaction field. This indicates a more correct reproduction of longer range orientational correlations. As a consequence, also the relative dielectric permitivity ϵ_r , as calculated from the Kirkwood-Fröhlich equation

$$\frac{(\epsilon_r - 1)(2\epsilon_r + 1)}{\epsilon_r} = \frac{g\mu^2}{\epsilon_o kT} \; G_K \quad ,$$

has the correct order of about 100 and shows an increase as observed experimentally /1/. For μ the electric dipole moment of the ST2-model μ = 2.35 D has been used.

There are also properties like the mean squared fluctuations of the temperature, where no marked temperature dependence can be observed within the present scatter. This can be understood by the fact that this quantity determins the specific heat at constant volume c_V , which does not increase monotonically with decreasing temperature, but passes through a flat maximum in the supercooled temperature region /1/. Furthermore the absolute value of c_V is in reasonable agreement with experimental values.

III.3 Average number of hydrogen bonds and fraction of molecules with j intact bonds

Within the framework of computer simulation, there are numerous possibilities for the definition of a hydrogen bond, varying from purely geometric to purely energetic, with many possible combinations. Earlier studies had shown that the result - the statistics of the hydrogen bond network structure - is not very sensitive to the details of the choice of the definition (see references in /12/). Therefore in our present study we use exclusively the following: Two molecules i and j are considered to be hydrogen bonded, if their interaction energy V_{ij} is stronger (more negative) than some chosen cutoff energy V_{HB} and their mutual oxygen-oxygen separation is less than 3.5 A. The question, which value has to be chosen for V_{HB}, can not be answered uniquely and will depend on the experiment, which one uses for comparison.

Due to this ambiguity, in previous studies each water configuration had been examined for a whole range of values V_{HB} , thus obtaining a series of pictures of the hydrogen bond network structure as it would reveal when going from very strict to very permissive definitions. Of course, the average number of hydrogen bonds per molecule $\langle n_{HB} \rangle$ will then vary also from nearly zero to about four.

Fig. 2 gives the dependence of $\langle n_{HB} \rangle$ on the definition threshold V_{HB}, obtained for the different simulation runs at various temperatures. In Figs. 5a and 6a below, vertical sections through this family of curves show $\langle n_{HB} \rangle$ as a function of temperature at fixed definition values V_{HB} . As one can see, the temperature dependence at constant density is very weak. This is in agreement with conclusion drawn from experimental data.

From the temperature dependence of the density at ambient pressure Stanley and Teixeira determined the fraction of intact hydrogen bonds p /4/; Luck /19/ and Walrafen /20/ obtained such values from infrared and raman spectroscopic data. They correspond to

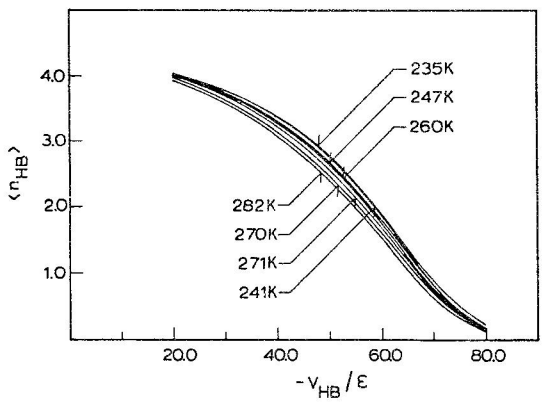

Fig. 2 : Average number of hydrogen bonds as a function of definition threshold V_{HB} (ε = 0.07575 kcal/mole) and temperature.

$\langle n_{HB} \rangle$-values, which we obtain, when choosing $-V_{HB}$ in the range of 2.5 to 3.5 kcal/mol. The MD-values show a weaker temperature dependence than the experimental ones, because the simulations are made at constant density ρ , whereas at constant pressure the density change promotes the formation of bonds, when decreasing the temperature

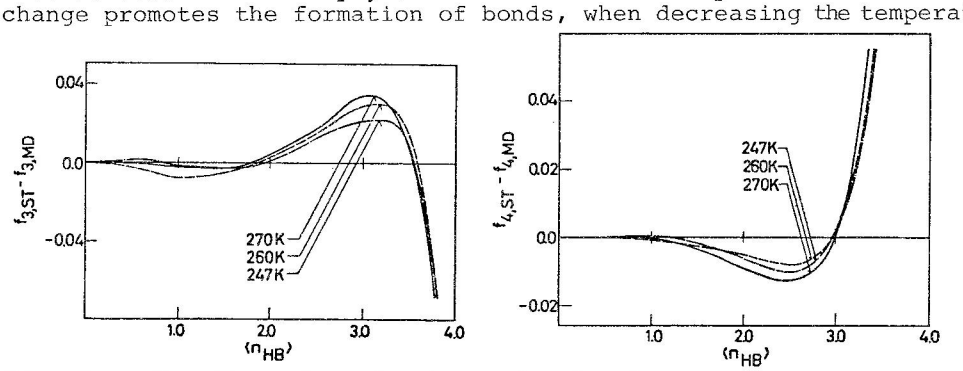

Fig. 3 : Fraction f_j of water molecules having exactly j intact hydrogen bonds (for j = 3 and 4) : Deviation of MD results $f_{j,MD}$ from binomial distribution $f_{j,ST}$.

As it was suggested by Stanley and Teixeira the fraction f_j of water molecules with exactly j intact bonds can be described by a binomial distribution law

$$f_j(p) = \binom{z}{j} p^j \, (1-p)^{z-j}$$

with $p = \langle n_{HB} \rangle / z$ and $z = 4$. Deviations can be observed only at very large p and for $j \geq 2$. Fig. 3 shows the deviations of the MD values $f_{j,MD}$ from the binomial distribution $f_{j,ST}$ for $j = 3$ and 4, and for different temperatures. These are very small below $\langle n_{HB} \rangle = 3$ and increase then rapidly /12/. As one can see, these deviations do not change very much with temperature. For f_3 a slight systematic improvement seems to be present. The very weak temperature dependence may be explained by two mechanisms, which are opposing each other : On the one hand temperature decrease will narrow distribution functions and favour tetrahedral local order, thus favouring a choice of $z = 4$. On the other hand the use of binomial distributions is based on the assumption of independent forming and breaking of bonds, which may become less valid with decreasing temperature. Here again, stronger effects may be visible when varying the density.

III.4 Size distributions $W_M^N(p)$ and $W_S^C(p)$

As discussed in sect. II, a quantitative agreement between the size distributions $W_M^N(p)$ and $W_S^C(p)$ from MD and the predictions of these quantities from percolation theory (using the assumption of random bond formation) could be demonstrated for ST2-water at 284 K. Fig. 4a shows the deviations of the MD simulation results $W_{M,MD}^N(p)$ from the predictions of percolation theory $W_{M,ST}^N(p)$ for two networks sizes $M = 3$ and 5 at three different temperatures. The same is given for the cluster size distributions $W_S^C(p)$ in Fig. 4b. Within the accuracy of our simulation results, a clear temperature dependence can hardly be extracted.

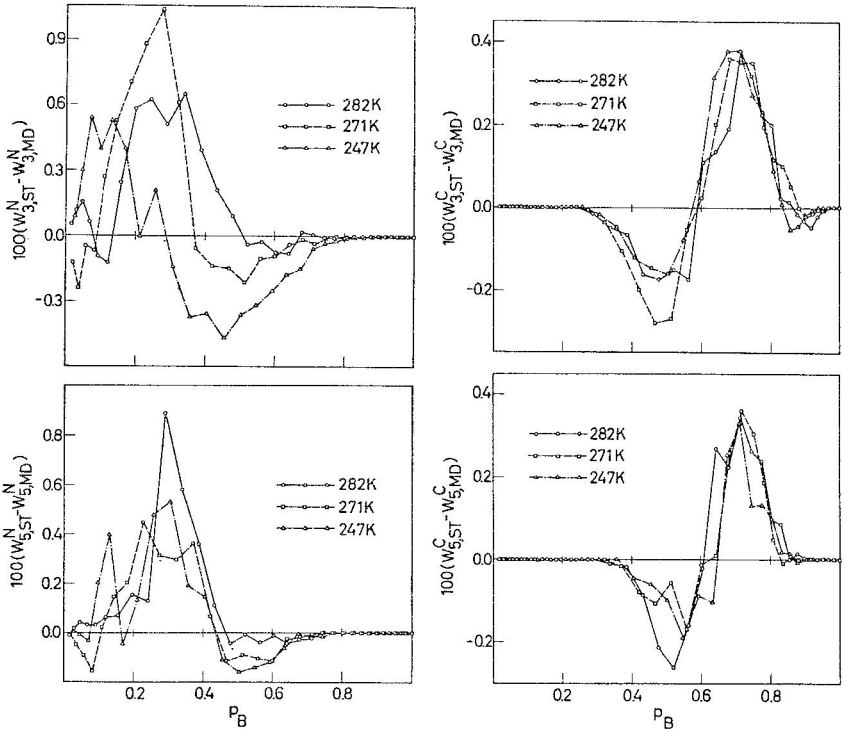

Fig. 4 : Size distribution of a.) bond networks W_M^N, b.) clusters of four-bonded molecules W_S^C : Deviation of MD results from percolation theory (ST) for network and cluster sizes M,s = 3 and 5.

It is very interesting that for W_S^C a systematic behavior of the deviations between MD results and predictions of correlated site percolation can be reproduced for all temperatures: for larger p we find positive deviations, for smaller p negative ones. As has been outlined earlier /12/, this parallels the behavior of the difference between the cluster size predictions from random site and from correlated site percolation theory. Even the positions of the transition points from positive to negative deviations are in close agreement. This had been interpreted as the manifestation of a weak additional cooperative effect, which leads - due to mutual stabilization of four-bonded molecules - to an increasing tendency of clumping together beyond the pure statistical correlation of sites as described by the correlated site percolation theory.

One could have expected that this tendency would increase with decreasing temperature, but this can not be confirmed here. Again, it might be that the influence of density will be much stronger than pure temperature influence. This will be studied in a simulation series, which is underway. On the other hand it should be noted that the coincidence between the curves for the different temperatures indicates clearly the validity of the temperature scaling approach, as it is implied in the percolation model.

III.5 Average network and cluster size S_N and S_C

In Fig. 5a and 6a the average hydrogen bond number $\langle n_{HB} \rangle$ is shown as a function of temperature for a series of definition valus V_{HB}. Fig. 6a presents the $\langle n_{HB} \rangle$ values below the bond percolation threshold at $\langle n_{HB} \rangle = 1.53$, whereas Fig. 5a contains those values below the site percolation point at $\langle n_{HB} \rangle = 3.18$. Variation of V_{HB} results only in a parallel shift of the curves, conserving the weak temperature dependence discussed before.

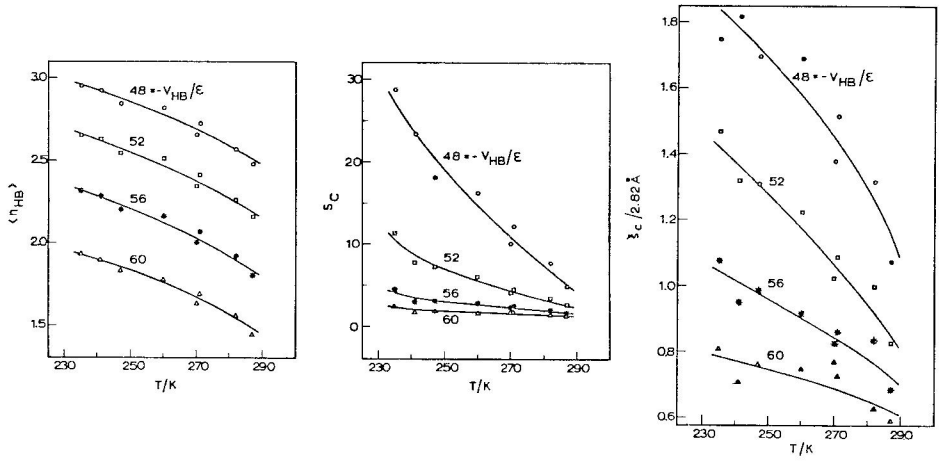

Fig. 5 : Temperature dependence of a.) average number of hydrogen bonds n_{HB} ; b.) average cluster size S_C, c.)spanning lenghts ξ_C (for different V_{HB}).

In contrast to this behavior, the temperature dependence of the average network and cluster sizes (summing only over finite size aggregates, omitting spanning ones):

$$S_C = \sum' s\, W_s^C \;/\; \sum' W_s^C$$

and $$S_N = \sum' M\, W_M^N \;/\; \sum' W_M^N$$

can not be described by parallel shifts, when changing V_{HB} (Figs. 5b and 6b). Rather, the increase of these quantities with decreasing

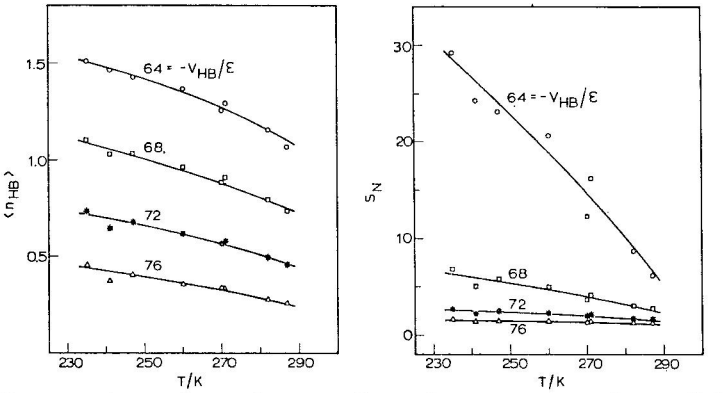

Fig. 6 : Temperature dependence of a.) average number of hydrogen bonds $\langle n_{HB} \rangle$, b.) average bond network size S_N (for different V_{HB}).

temperature becomes much more accelerated, when approaching the percolation threshold. Unfortunately, the statistical accuracy of the large cluster sizes is not very high and finite size effects are leading to systematic errors (like for example the convexe curvature of $S_N(T)$. Moreover, there are not enough temperature values to test a scaling law dependence. Additionally, Fig. 5c gives the average "spanning lenght" of these clusters (for definition see /16/). Again, an accelerated increase can be seen, when the corresponding $\langle n_{HB} \rangle$ values are approaching the percolation threshold.

III.6 Fluctuation of "local density" and structure factor S(Q)

As discussed in section II, we had shown earlier for a ST2 water system at T = 284 K that the local density is decreased in the vicinity of water molecules with four intact hydrogen bonds /13/. For this purpose the difference

$$\Delta n(R_O) = n_{<}(R_O) - n_4(R_O)$$

is calculated, where $n_4(R_O)$ is the average number of neighbors, which one finds within a sphere of Radius R_O around four-bonded water molecules. $n_{<}(R_O)$ is the same quantity for molecules with less than four bonds. All distances R_O refer to oxygen-oxygen separations.

Of course Δn varies with R_O, but also with the applied hydrogen bond definition value V_{HB}. The results are shown for three different temperatures (T = 270 K, 260 K and 247 K) in the upper row of Fig. 7. The qualitative picture is the same as obtained for the earlier T = 284 K system: there are oscillations of $\Delta n(R_O)$ due to the oscillatory nature of the oxygen-oxygen pair correlation function $g_{OO}(r)$, but more important is the fact that these oscillations

are not symmetric around the zero line but seem to approach a positive limiting value for large R_o . This effect becomes more pronounced, when using a more strict definition for the hydrogen bond.

From Fig. 7 we can see that at constant V_{HB} the density difference as measured by $\Delta n(R_o)$ becomes more pronounced, when lowering the temperature. As this is in agreement with the results of small angle x-ray scattering experiments, we did also calculate from the distribution of the oxygen positions the scattering function

$$S(Q) = \frac{1}{N} \cdot \left\langle \sum_{k,l} \exp\ (i\ \underline{Q}\ \underline{R}_{kl}) \right\rangle ;$$

where the sum includes all pairs of molecules k an l and $\underline{R}_{kl}$ is the corresponding oxygen distance vector. From scattering vectors with $|Q|>1.2$ Å^{-1} , S(Q) can be calculated by Fourier-transforming the oxygen pair correlation function $g_{OO}(r)$. For smaller Q values S(Q) has been calculated directly from the above sum. As the box size of our MD systems is L = 18.63 Å , the smallest accesible wave vetor is $Q_1 = 2\pi/L = 0,34$ Å^{-1} . One can see from Fig. 7 that with decreasing temperature an increase of S(Q) at low Q values is developing with a minimum between 0.5 and 1.0 Å^{-1} .This is in qualitative agreement with the above mentioned experimental findings and has been interpreted by the presence of density fluctuations with correlation lenghts of the order of 8 Å /14/.

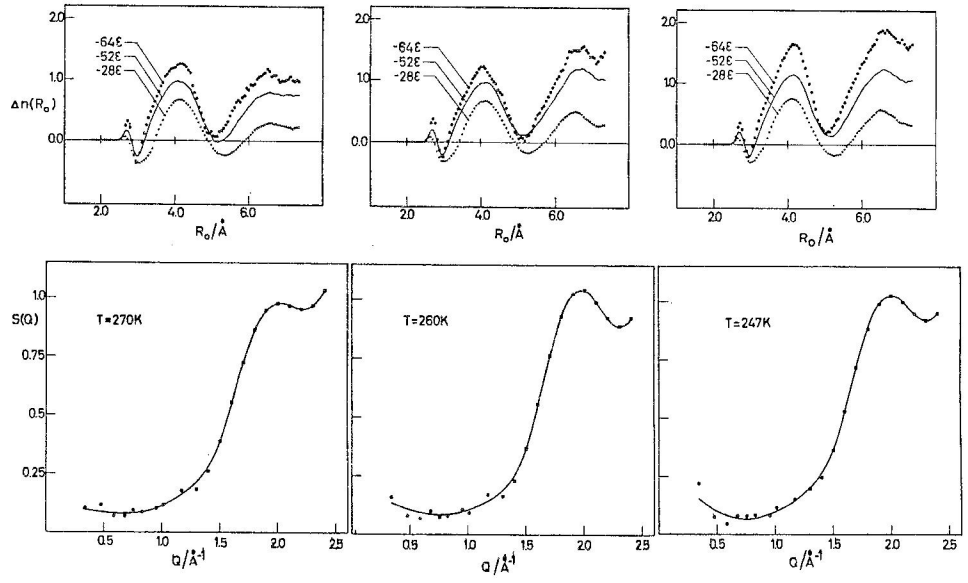

Fig. 7 : Difference in local density around four-bonded and non-four-bonded molecules at T = 270, 260 and 247 K (upper row), structure factor S(Q) for low wave vectors Q (below)

An extrapolation of the S(Q) curves leads to compressibilities,which are roughly a factor of two larger than the experimental values (in agreement with Rahman and Stillingers data for ST2 water), but which show the experimentally observed temperature variation.

From Fig. 8 one can see that this increase at low Q values is real

and not due to some statistical deviations. The upper part shows the time development of $S(Q)$ for the lowest Q value $Q_1 = 2\pi/L$ at $T = 247$ K over a very long equilibration period of 120 ps. In contrast to $S(Q)$ for $Q_2 = \sqrt{2} \cdot 2\pi/L$ below, a clear increase is visible. The inserts show $\Delta n(R_o)$ averaged over time intervals at the beginning and at the end of the equilibration period (indicated by horizontal bars below and above).

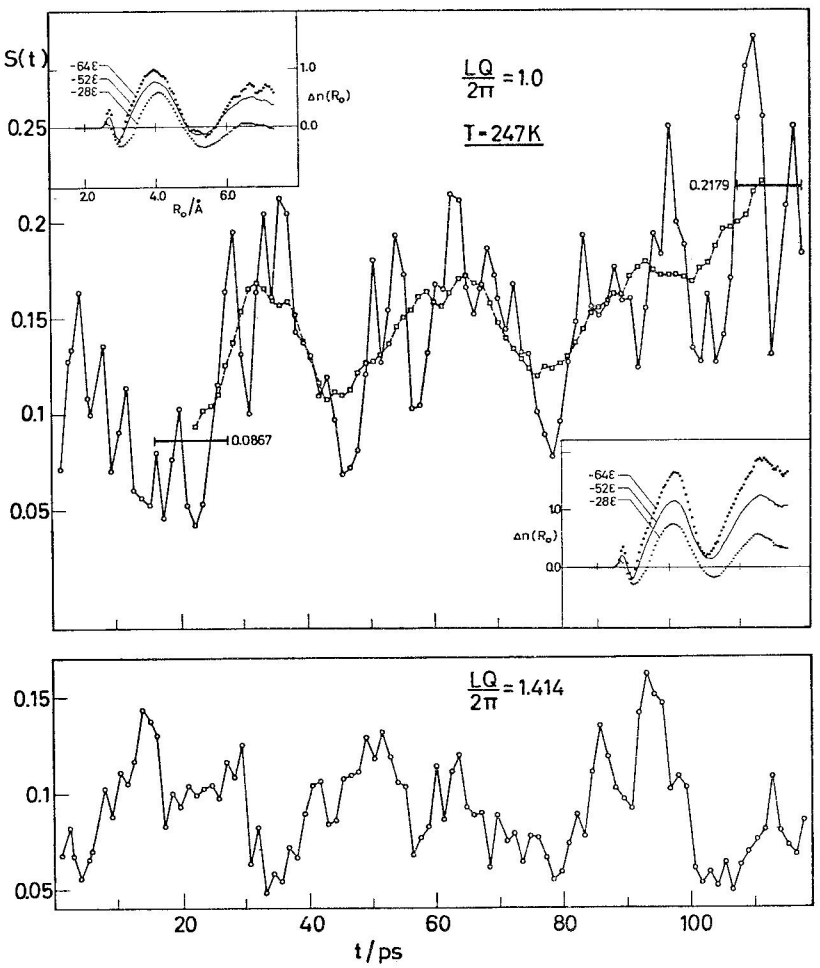

Fig. 8 : Time evolution of $S(Q)$ for the two lowest accessible wave vectors. Inserts: Density differences monitored during time intervals marked by horizontal lines below and above.

A correlation between the discussed density difference and the raising $S(Q)$ can be observed. The full curve displays $S(Q)$ values averaged over 500 consecutive configurations, whereas the smoother dashed curve corresponds to $S(Q)$ averages over longer time intervals (2000 timesteps).

In addition to high frequency fluctuations also long range structural fluctuations with characteristic periods of roughly 20 ps seem to be present.

III.7 Local density and binding energy

Recently we could identify an 'unusual' correlation between local density and 'binding energy' of the water molecules (see section II), demonstrating an energetic preference for loose packing.

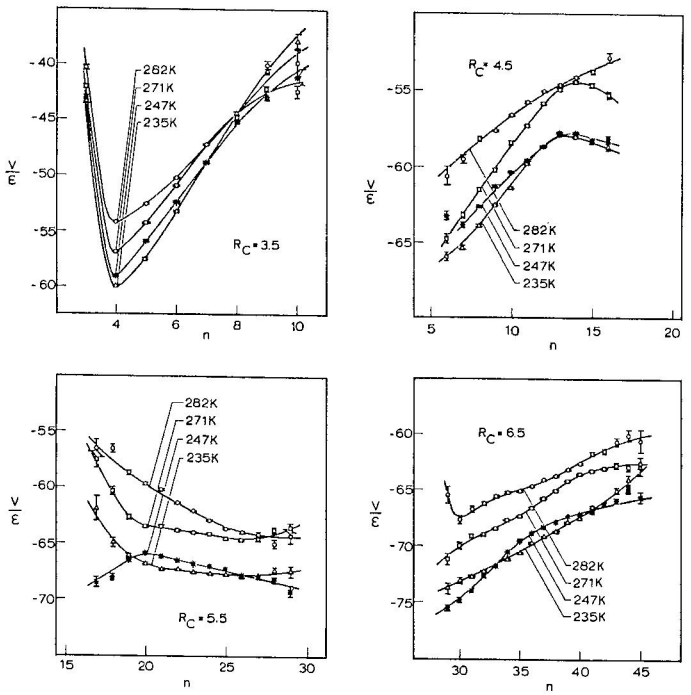

Fig. 9 : Correlation between the number of neighbors within spheres of radius R_C = 3.5 to 6.5 Å and the average interaction energy of the central particle.

In Fig. 9 we can see the temperature dependence of this relation. There, the average binding energy

$$V(n) = \langle V_j \rangle_{n=const.} = \left\langle \sum_{i \neq j}^{n} V_{ij} \right\rangle$$

is given as a function of the number of neighbors n, which one finds within a cutoff-sphere with R_C = 3.5, 4.5, 5.5 and 6.5 Å respectively and which contribute to V_j.

As one can see for R_C = 3.5 Å, there is a strong energetic preference for four neighbors. A decrease of temperature is amplifying

this tendency. Also, for R_c = 4.5 and 6.5 Å the 'unusual' increase of V(n) with increasing number of neighbors is conserved; the temperature decrease leading again to a lowering of the curves. The 'normal' decrease of V with n, found for R_c = 5.5 Å and higher temperatures is converted into a very flat dependence at lower temperatures.

IV. TEMPERATURE DEPENDENCE OF DYNAMIC PROPERTIES

IV.1 Self diffusion and reorientation

Self diffusion coefficients have been calculated from the long time slope of the mean squared displacement of the water molecules. In Fig. 10 they are compared with the experimental data of Gillen et al. (nmr spin-echo measurements at 1 bar pressure) corrected by Angell /1,21/. As mentioned in section II, due to the application of the reaction field method, the MD results show a higher mobility. Although at higher temperatures both sets of data run in parallel, this is not true for lower temperatures, where the experimental (constant pressure) line shows an accelerated increase. In our constant density

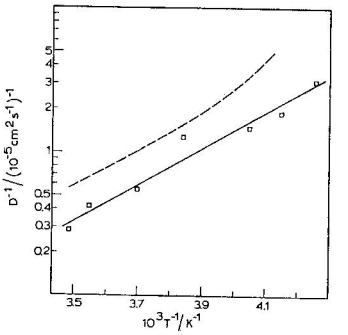

Fig. 10 :
Temperature dependence of the self-diffusion coefficient. Dashed line: experimental results, squares: MD results.

simulation series the pressure increases with decreasing temperature, leading to a weaker temperature dependence, in accord with experimental findings.

The reorientational motion has been studied by calculating time autocorrelation functions $T_1'(t)$ for Legendre Polynomials $P_1(\cos\Theta)$ of different molecule fixed unit vectors $\hat{\mu}_i$:

$$T_1'(t) = \langle P_1 (\hat{\mu}_i (t_o) \cdot \hat{\mu}_i (t_o+t)) \rangle .$$

As observed earlier, these functions show initially a fast librational decay which is followed by an exponential decline at long times. Correlation times τ_1 have been obtained by integrating $T_1'(t)$ up to t = 4 ps and assuming an exponential decay for $t \longrightarrow \infty$ with the average slope of $\ln T_1'(t)$ between 2 and 4 ps.

In Fig. 11 a,b τ_1 for the electric dipole vector reorientation and τ_2 for the dipole vector and the proton-proton connection vector are given as a function of temperature. τ_1 is compared with the dielectric relaxation time τ_D of Bertolini et al. /22/ which has been claimed to be identical with the single particle reorientation time τ_1 /23/. τ_2 is compared with the corresponding value obtained by Lang and Lüdemann for the OH-bond reorientation /3/.

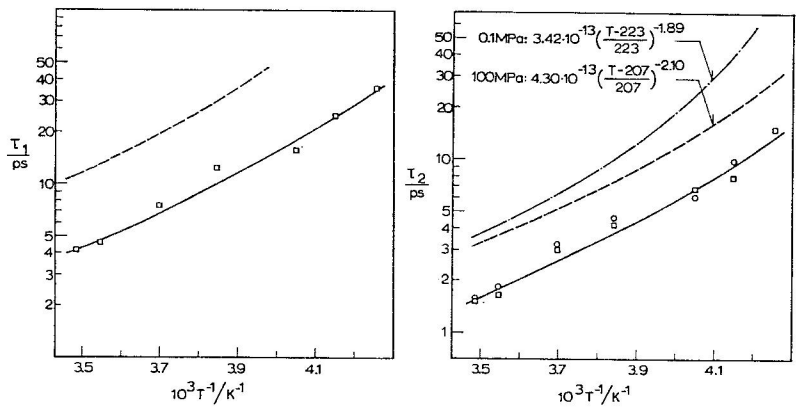

Fig. 11 : Temperature dependence of reorientational correlation times τ_1 and τ_2 from MD (squares and circles) and experiments (dashed lines).

One can see that within the appreciable scatter of our reorientation times, the MD values run in parallel to the experimental values. In particular, the curvature of the MD line for τ_2 is closer to the 100 MPa curve of Lang and Lüdemann, in accord with the increasing pressure in our simulation.

The absolute values of the MD simulation seem to be much too low compared to the experimental ones. But recent nmr relaxation studies of the ^1H - ^{17}O interaction in water also suggest lower values /24,25/. For example at 25°C Sposito /23/ calculated from Bertolini et al.'s data τ_2 = 2.85 ps, Lang and Lüdemanns 1 bar-formula gives τ_2 = 2.68 ps, whereas the above mentioned new studies yield τ_2 = 1.7 to 1.9 ps, which would be much closer to our simulation values.

IV.2 Hydrogen bond lifetimes

The lifetime of hydrogen bonds plays an important role in the interpretation of light scattering experiments /26-28/ as well as in several theoretical approaches to understand the dynamics of water molecules /29,30/. There are also two preliminary MD studies of this quantity /31,32/.

Just as there is no unique way to distinguish unambiguously between broken and intact hydrogen bonds, there exist many different possibilities for the definition of a hydrogen bond lifetime. Based on a hydrogen bond definition similar to the one we use here, Stillinger /33/ has proposed three distinct lifetime "queries", of which we will adopt here the most rigorous one.

Every eight MD timesteps ($\approx$ 0.01 ps) we record all hydrogen bonds. Then we measure for each individual bond the time between its first appearance and the breaking of the bond. This gives us a histogram

h(t) of observed lifetimes: the number of pairs of molecules, which have an uninterrupted bond for a time period t . Of course, we can not registrate intermittent interruptions. On the other hand, if the bond has been broken for only one observation time, the lifetime count starts from zero again. Concerning different kinds of possible experiments to measure lifetimes, each one will have a finite resolution of observation times, overlooking short breaks. Thus our definition is quite strict, delivering values near the lower boundary of observable lifetimes.

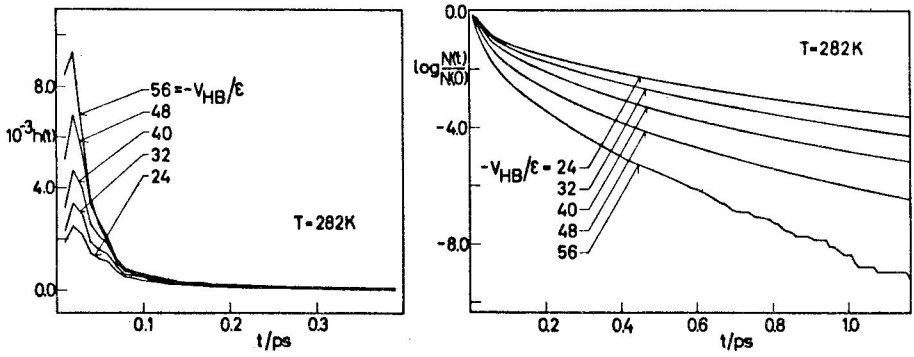

Fig. 12 : a) histogram of observed hydrogen-bond lifetimes, b) logarithm of the decay function N(t) / N(o).

Fig. 12a shows some histograms h(t) for the system at T = 282 K and several V_{HB} values. Like Tanaka et al. /31/ we observe maxima near $t \approx 2 \cdot 10^{-14}$ s. But in contrast to these authors we do not interpret this time as being characteristic for the lifetime of the hydrogen bonds, because the occurence of the maxima is just due to the librational motion of the molecules. This can be seen from the fact that Rahman and Stillinger /8/ observed a high frequency peak in the spectrum of the rotational motion near $\omega = 16 \cdot 10^{13}\ s^{-1}$, which corresponds to half periods of $2 \cdot 10^{-14}$ s.

From the histogram of lifetimes h(t) we calculate the number of bonds which are still unbroken after a time t , the "decay function"

$$N(t) = \int_t^\infty h(t')\, dt'$$

(see Fig. 12b). We find a nonexponential decay and define an average lifetime by

$$\tau_{HB} = \frac{1}{N(o)} \int_o^\infty N(t)\, dt \ .$$

N(t) is determined for times up to 1.2 ps. Except for very small values of $-V_{HB}$ then h(t) has decreased practically to zero and the numerical integration can be carried out. In the other cases, the slope of ln N(t) near $t \approx 1$ ps is determined and an exponential continuation is assumed. In Fig. 13a the dependence of τ_{HB} from the definition value V_{HB} is shown for the two extreme temperatures of our simulation runs, together with τ_{ls} , which characterizes the slope of ln N(t) at long times. As one can see, there is a very weak

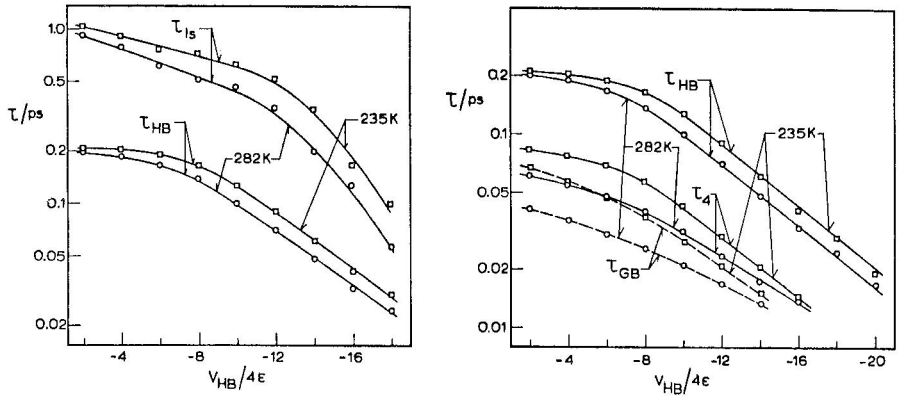

Fig. 13 : a) Average hydrogen bond lifetime τ_{HB} and longtime slope τ_{1s} of ln N(t),
b) comparison with average lifetime of four-bonded molecules τ_4 and of bonds between four-bonded molecules τ_{GB} .

temperature dependence and τ_{HB} becomes very short at strict definitions. The negative curvature at low values of $-V_{HB}$ probably stems from edge effects due to the finiteness of our simulation runs.

In the same way as we obtained τ_{HB} , we also calculated the lifetime of four-bonded water molecules τ_4 and the lifetime of hydrogen bonds between two four-bonded water molecules τ_{GB} . In Fig. 13b these are compared again for the two extreme temperatures with τ_{HB} . In our definition, the lifetime of a four-bonded molecule ends, when at least one of the four bonds of that molecule breaks; similiarly at least one out of seven bonds has to break, to make vanish the bond between two four-bonded molecules. As we can see from Fig. 13b τ_4 and τ_{GB} are longer than just one fourth ore one seventh of τ_{HB} , as one would expect for example for simple independent Markoff processes.To what extend this deviation is due to the presence of cooperativity in the bond formation process has to be clarified in a more detailed study.

Finally, in Fig. 14 the temperature dependence of τ_{HB} and τ_4 for some selected fixed values of V_{HB} is compared with the temperature dependence of τ_2 from Fig. 11b. Note that there is a gap of one decade in the ordinate. As one can see, the temperature dependence of τ_{HB} and τ_4 is much weaker than that of τ_2. The same difference in temperature dependence we found in section III.5 (see Figs. 5 and 6) for some static quantities, when we compared the single bond property $\langle n_{HB} \rangle$ with the characteristic size S of bond networks. This parallelism suggests a strong influence of the network properties on the single molecule dynamics and has to be investigated further.

A comparable difference in the temperature dependence of reorientation times and time constants which are assigned to the hydrogen bond lifetime could be observed experimentally /28/, although our τ_{HB} values are much shorter and show very small activation energies ($\approx$1 kcal/mol). This can be explained by the previously discussed very strict definition, which we use and which should deliver a lower bound for the experimentally observable times. Note also, that τ_{1s} delivers

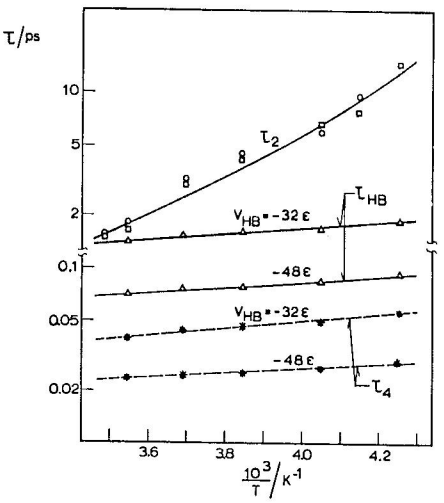

Fig. 14 : Temperature dependence of reorientation correlation time τ_2 compared to τ_{HB} and τ_4 for different V_{HB}.

higher values, which are comparable to the experimental ones. Presently, we are testing other definitions of hydrogen bond lifetimes, in particular allowing intervening interruptions /33/.

V. CONCLUSIONS

We are studying the hydrogen bond connectivity and dynamics of "ST2-water", a model liquid, which shows many - if not all - of the anomalies of "real" water. To isolate pure temperature from density effects, we made a series of simulation runs at constant volume. As expected, when penetrating the region of the supercooled liquid, increasing low frequency fluctuations lead to growing difficulties in getting statistically significant results. Nevertheless, we could show that the pure temperature influence on single bond properties (static as well as dynamic ones) is very weak, whereas many-particle quantities like cluster sizes or network influenced properties like reorientation and self diffusion of the molecules show an accelerated temperature variation.

The present results suggest that pure density effects might have a stronger influence on the observed properties. This will be investigated in a simulation series, which is underway.

Financial support by ONR, ARO, NSF, Stiftung Volkswagenwerk and Fonds der Chemischen Industrie is gratefully acknowledged.

REFERENCES :

1/ C.A. Angell in "Water - A Comprehensive Treatise", Vol. 7, Chapter 1. F. Franks, Ed., Plenum Press, New York, 1983
2/ C.A. Angell,Ann.Rev.Phys.Chem. 34, 593 (1983)
3/ E.W. Lang and H.-D. Lüdemann, Angew. Chemie, Intern.Ed. 21, 315 (1982)
4/ H.E. Stanley, J. Phys. A 12, L 329 (1979) ;
H.E. Stanley and J. Teixeira, J. Chem. Phys. 73, 3404 (1980) ;
H.E. Stanley, J. Teixeira, A. Geiger and R.L. Blumberg, Physica 106A, 260(1981)

5/ F.H. Stillinger, Science 209, 451 (1980)
6/ F.H. Stillinger in "Water in Polymers", S.P. Rowland, Ed., ACS Symposium, Seris No. 127, Am. Chem. Soc. Washington D.C. (1981)
7/ R. Speedy, preprint 1983
8/ A. Rahman and F.H. Stillinger, J. Chem. Phys. 55, 3336 (1971)
9/ F.H. Stillinger and A. Rahman, J. Chem. Phys. 60, 1545 (1974)
10/ A. Rahman and F.H. Stillinger, J. Am. Chem. Soc. 95, 7943 (1973)
11/ A. Geiger, F.H. Stillinger,and A. Rahman, J. Chem. Phys. 70, 4185 (1979)
12/ R.L. Blumberg, H.E. Stanley, A. Geiger, and P. Mausbach, J. Chem. Phys. 80, 5230 (1984)
13/ A. Geiger and H.E. Stanley, Phys. Rev. Lett. 49, 1749 (1982)
14/ L. Bosio, J. Teixeira, and H.E. Stanley, Phys. Rev. Lett. 46, 597 (1981)
15/ H.E. Stanley, R.L. Blumberg, and A. Geiger, Phys. Rev. B 28, 192€ (1983)
16/ A. Geiger and H.E. Stanley, Phys. Rev. Lett. 49, 1895 (1982)
17/ O. Steinhauser, Mol. Phys. 45, 335 (1982)
18/ W.F. van Gunsteren, H.J.C.Berendsen, and J.A.C. Rullmann, Faraday Disc. 66, 58 (1978)
19/ W.A.P. Luck and W. Ditter, Z. Naturforsch. 24b, 482 (1969)
20/ G.E. Walrafen in "Water - A Comprehensive Treatise", Vol. 1, Chapter 5, F. Franks, Ed., Plenum , N.Y., 1972
21/ K.T. Gillen, D.C. Douglas, and M.J.R. Hoch, J. Chem. Phys. 57, 5117 (1972)
22/ D. Bertolini, M. Cassettari, and G. Salvetti, J. Chem. Phys. 76, 3285 (1982)
23/ G. Sposito, J. Chem. Phys. 74, 6943 (1981)
24/ D. Lankhorst, J. Schriever, and J.C. Leyte, Ber. Bunsenges. Phys. Chem. 86, 215 (1982)
25/ B. Gordalla, M.D. Zeidler, private communication
26/ C.J. Montrose, J.A. Bucaro, J. Marshall, and T.A. Litovitz, J. Chem. Phys. 60, 5025 (1974)
27/ W. Danninger and G. Zundel, J. Chem. Phys. 74, 2769 (1981)
28/ O. Conde and J. Teixeira, J. Physique 44, 525 (1983)
29/ H.G. Hertz and M.D. Zeidler in "The Hydrogen Bond", Vol. 3, Chapter 21, P. Schuster, G. Zundel, and C. Sandorfy, Eds., North Holland, Amsterdam 1976
30/ D. Bertolini, M. Cassettari, M. Ferrario, G. Salvetti, and P. Grigolini, Chem. Phys. Lett. 98, 548 (1983)
31/ H. Tanaka, K. Nakanishi, and N. Watanabe, J. Chem. Phys. 78, 2626 (1983)
32/ D.C. Rapaport, Mol. Phys. 50, 1151 (1983)
33/ F.H. Stillinger, Advances Chem. Phys. 31, 1 (1975).